doi:10.1016/j.jmb.2007.05.089 J. Mol. Biol. (2007) xx, xxx–xxx

JMB

Available online at www.sciencedirect.com
ScienceDirect

ELSEVIER

Structural Characterization of the Ceruloplasmin: Lactoferrin Complex in Solution

Annalaura Sabatucci[1], Patrice Vachette[3,4], Vadim B. Vasilyev[5] Mariano Beltramini[2], Alexey Sokolov[5], Maria Pulina[5] Benedetto Salvato[2], Clotilde B. Angelucci[1], Mauro Maccarrone[1] Ivo Cozzani[1] and Enrico Dainese[1]*

[1]*Department of Biomedical Sciences, University of Teramo Teramo, Italy*

[2]*Department of Biology University of Padova Padova, Italy*

[3]*CNRS, IBBMC UMR 8619 -Orsay F-91405, France*

[4]*University Paris-Sud Orsay, F-91405, France*

[5]*Institute for Experimental Medicine, Saint-Petersburg 197376, Russia*

**Corresponding author*

Ceruloplasmin is a copper protein found in vertebrate plasma, which belongs to the family of multicopper oxidases. Like transferrin of the blood plasma, lactoferrin, the iron-containing protein of human milk, saliva, tears, seminal plasma and of neutrophilic leukocytes tightly binds two ferric ions. Human lactoferrin and ceruloplasmin have been previously shown to interact both *in vivo* and *in vitro* forming a complex. Here we describe a study of the conformation of the human lactoferrin/ceruloplasmin complex in solution using small angle X-ray scattering. Our *ab initio* structural analysis shows that the complex has a 1:1 stoichiometry and suggests that complex formation occurs without major conformational rearrangements of either protein. Rigid-body modeling of the mutual arrangement of proteins in the complex essentially yields two families of solutions. Final discrimination is possible when integrating in the modeling process extra information translating into structural constraints on the interaction between the two partners.

Keywords: human lactoferrin; human ceruloplasmin; conformation in solution; complex; SAXS

Introduction

Ceruloplasmin (ferro-O_2-oxidoreductase, EC 1.16.3.1, hCp) is a protein that belongs to the family of multicopper oxidases (MCOs) and accounts for 95% of human plasma copper. Cp is believed to play an important role in iron metabolism and homeostasis as it allows the incorporation of Fe^{3+} into apotransferrin.[1–5] The homolog of human Cp (hCp), Fet3p from *Saccharomyces cerevisiae*, also possesses a ferroxidase activity that, in a complex with an iron permease (Ftr1p), allows the iron uptake from the extracellular environment.[6] The recent resolution of the crystal structure of this ancestor ferroxidase further underlies the key role of the copper-iron biochemical connection in the trafficking of iron in diverse eukaryotic organisms.[7]

An internal triplication within the single chain of hCp consisting of 1046 amino acid residues has been proposed upon resolving its primary structure.[8,9] It was shown later that six homologous domains of hCp are arranged in three pairs forming a triangular array around a pseudo 3-fold symmetry axis as revealed by its X-ray structure resolved at 3.1 Å.[10] Structural similarities of Cp with other copper-containing proteins allowed proposing its evolutionary descent from a plastocyanin-like ancestor[11] and a common pattern for all the so-called cupredoxins, a group including the MCOs (Cp, laccase, ascorbate oxidase) and nitrite reductase.[10,12–15] Three different types of copper ions have been distinguished in MCOs on the basis of their spectroscopic features. In hCp different amino acid ligands from several domains coordinate six copper atoms, endowing them with different spectroscopic properties. Domains 2, 4 and 6 each contain a mononuclear type 1 copper atom, while a trinuclear cluster composed of the only type 2 copper atom and of two

Abbreviations used: SAXS, small angle X-ray scattering; hCp, human ceruloplasmin; hLf, human lactoferrin; SE-HPLC, size-exclusion high pressure liquid chromatography.

E-mail address of the corresponding author: edainese@unite.it

Please cite this article as: Sabatucci, A. *et al.*, Structural Characterization of the Ceruloplasmin: Lactoferrin Complex in Solution, *J. Mol. Biol.* (2007), doi:10.1016/j.jmb.2007.05.089

type 3 atoms is located at the interface between domains 1 and 6 and coordinated by amino acids from both domains.[10] Recently, evidence for a structural role of the type 3 copper ions in the stabilization of the tertiary structure of the native hCp has been obtained using small angle X-ray scattering (SAXS).[16]

Human lactoferrin (hLf) is a basic (p*I* 8.6) glycoprotein, which consists of a single polypeptide chain that is folded in two highly homologous lobes, namely the N and C-lobe. Like other proteins of the transferrin family, Lf is involved in the control of iron levels through its very tight, but reversible binding of iron in a Fe^{3+}-binding site contained in each lobe.[17–19] HLf is expressed and secreted by glandular epithelial cells and is found in the secretory granules of neutrophils. While iron binding seems to be central to the role of this protein in iron homeostasis, other activities contribute to the pleiotropic functional nature of Lf. These can be summarized as follows: regulation of cellular growth and differentiation,[20] host defense against a broad range of microbial infections,[21] anti-inflammatory activity, and protection against cancer development and metastasis.[22,23] Accomplishing its biological functions Lf displays versatile capacities, such as specific interactions with microbial species or binding to receptors of mammalian cells. In addition, Lf is known to interact with various proteins in mammalian organisms such as calmodulin[24] and some secretory proteins[25,26], and to bind to the protein receptors on bacterial cell surfaces.[21,27] The positively charged N-terminal domain of hLf is involved in different functions of the protein and is responsible for the interaction with negatively charged ligands, such as bacterial lipopolysaccharides, DNA and heparin;[28–31] with other proteins such as human lysozyme[28] and with specific receptors.[32–34] In contrast, the C terminus of hLf has been identified to be responsible for its interaction with specific bacterial receptors (Lbpa).[27]

Recently it has been reported that Cp and Lf interact both *in vivo* and *in vitro* to form a stable complex,[35,36] with a dissociation constant K_d determined as 1.8×10^{-6} M.[35] It was also demonstrated that hLf binding to hCp *in vitro* increases the ferroxidase activity of the latter.[37] This activity was later found *in vivo* in the hCp:hLf complex of breast milk.[36] The interaction between hLf and hCp is not accompanied by major tertiary structure changes in either protein as demonstrated by the near-UV CD data obtained on the hCp:hLf complex.[35] In addition, the hCp:hLf interaction has been proposed to have a marked electrostatic character, with a suggested involvement of the arginine ^{2}R-R-R-R^{5} positive cluster at the N terminus of hLf and a negatively charged stretch in the C terminus of hCp.[36–38] This was supported by the evidence that salmon protamine mimicking the N terminus of hLf as well as synthetic R-R-R-R peptide cause dissociation of the hCp:hLf complex.[36,39] The stoichiometry of the hCp:hLf complex may be questioned as both 1hCp:2hLf and 1hCp:1hLf complexes have been suggested to be present *in vitro*, while only a 1:1 species was found *in vivo*.[36,38]

We report here a study of the hCp:hLf complex using both size-exclusion chromatography (SE-HPLC) and SAXS in order to obtain direct information on the stoichiometry and to analyze its overall conformation in solution. The effects of chaotropic and kosmotropic solutions on the complex formation and aggregation have been also analyzed.

SAXS provides information on the overall conformation of proteins in solution[40,41] and has been recently successfully applied to study protein complexes.[42–44] Furthermore, SAXS has been recently proposed as one of the useful biophysical techniques providing structural information on biomolecular complexes that can be used as constraints in data-driven docking programs.[45]

Our SAXS study, supporting previous biochemical data, gives direct evidence that in solution the two proteins interact forming exclusively a complex with a 1:1 stoichiometry, according to a well-defined geometry. In addition, from an *ab initio* analysis of the overall structure of the complex and rigid-body modeling, we infer some information about the regions of interaction of the two proteins. Our data are compatible with a recently proposed model for the interaction involving the N-terminal region of hLf and the C-terminal region of hCp.[36–38]

Results

Structural characterization of pure hLf and hCp in solution

As hLf tends to self-aggregate in solution leading to the formation of tetramers, the stability of which is dependent on the ionic strength of the solution,[46] we first used buffers at different pH and ionic strength (see Materials and Methods) to define the best experimental conditions to stabilize the monomeric form of the protein. Using a 50 mM Tris-HCl buffer (pH 7.0) in the presence of 100 mM NaCl, we obtained by SE-HPLC analysis a single peak for hLf (Figure 1, dotted line) with an elution volume corresponding to a molecular mass of 85(±9) kDa. In the same buffer, hCp also eluted as a single peak corresponding to a molecular mass of 118(±12) kDa (Figure 1, broken line). Thus obtained, hLf was analyzed by SAXS. The resulting scattering pattern of hLf in solution is presented in Figure 2 (dotted line). The concentration *c* (2.7 mg/ml) was sufficiently low to make interparticle interactions negligible in the buffer used. The value of the radius of gyration of hLf calculated using the Guinier approximation is $R_g = 32.0(\pm 1)$ Å. From the analysis of the pair distribution function, ($p(r)$) (Figure 3, dotted line), the maximum dimension of the particle (D_{max}) has a value of 100(±10) Å, and the calculated value of radius of gyration in the real space is $R_g = 32.9(\pm 0.3)$ Å, in good agreement with the Guinier estimate (see also Table 1). The fitting of the theoretical curve obtained from the crystal

Please cite this article as: Sabatucci, A. *et al.*, Structural Characterization of the Ceruloplasmin: Lactoferrin Complex in Solution, *J. Mol. Biol.* (2007), doi:10.1016/j.jmb.2007.05.089

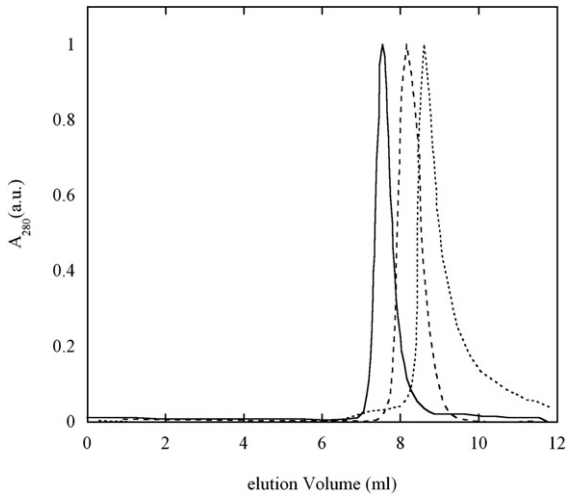

Figure 1. SE-HPLC peaks of pure hLf in 50 mM Tris-HCl (pH 7.0) buffer in the presence of 100 mM NaCl (dotted line); of pure hCp (broken line) and 1:1 hCp:hLf complex (continuous line).

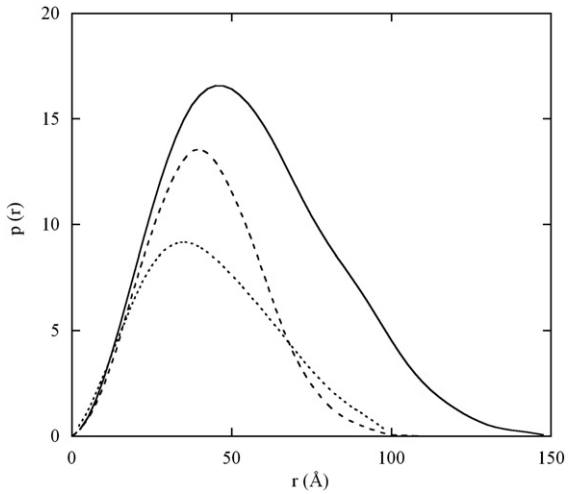

Figure 3. Comparison of the $p(r)$ functions of hLf (dotted line), of hCp (broken line), and of the complex (continuous line).

structure of recombinant holo hLf (1B0L.pdb)[47] agrees well with the experimental pattern as shown in Figure 4.

The conformations in solution of both the holo and the apo form of hCp have already been reported.[16] The structural parameters of holo hCp are summarized in Table 1, the experimental scattering pattern is reported in Figure 2 (broken line), and the calculated pair distribution function $p(r)$ in Figure 3 (broken line).

Structural parameters of the hCp:hLf complex

The hCp:hLf complex was obtained by directly mixing the two proteins previously equilibrated in 50 mM Tris-HCl buffer (pH 7.0) both in a 1:1 and in a 1:2 molar ratio. No salt was added to the solution since 300 mM NaCl is known to dissociate the complex.[38] The solution containing hCp and hLf in a 1:2 molar ratio eluted as two peaks in SE-HPLC. The first peak eluted at a volume corresponding to a calculated molecular mass of 230(±23) kDa, in close agreement with the theoretical value (~210 kDa) expected for a hCp:hLf complex with a 1:1 stoichiometry and with the experimental data on gel filtration on Toyopearl HW-55 of hCp:hLf complex from breast milk, which yielded the value 220 (±10) kDa.[36] The second peak, with a molecular mass of 85(±9) kDa, corresponded to free hLf that was in excess and did not interact with hCp (data not shown). In agreement with the previous analysis, the solution containing a mixture of hCp:hLf in a molar ratio 1:1 gave rise to a chromatographic profile showing only a single peak (Figure 1, continuous line), with a determined molecular mass matching that of the first peak obtained when the proteins were mixed in a 1:2 molar ratio. The SAXS patterns of the proteins contained in isolated peaks of the complex formed either at hCp:hLf molar ratio 1:1 or 1:2 were practically identical (data not shown), showing that the conformation of the complex was the same for both values of the initial molar ratio. In order to check whether the SE-HPLC separation could favor the dissociation of a putative 1:2

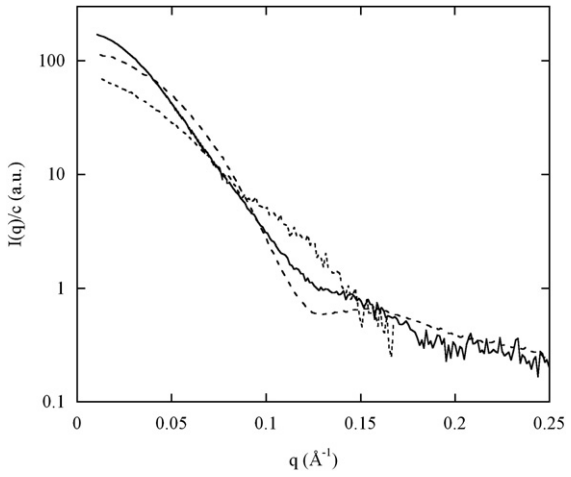

Figure 2. Experimental SAXS patterns of hLf (dotted line), of hCp (broken line), and of the complex (continuous line).

Table 1. Structural parameters of isolated proteins (hCp and hLf) and of the complex derived from SAXS patterns

Sample	R_g (Å) Guinier	$I(0)/c$ ratio	M_r ratio[a]	R_g (Å) $p(r)$	D_{max} (Å)
hLf	32.0±1	1	1	32.9±0.3	100±10
hCp	32.5±0.5	1.78	1.71	32.3±0.2	110±5
Complex	42.8±1	2.78	2.71[b] 3.71[c]	43.8±0.3	150±5

[a] Calculated from the amino acid sequence.
[b] For a 1:1 stoichiometry.
[c] For a 1:2 stoichiometry.

Please cite this article as: Sabatucci, A. *et al.*, Structural Characterization of the Ceruloplasmin: Lactoferrin Complex in Solution, *J. Mol. Biol.* (2007), doi:10.1016/j.jmb.2007.05.089

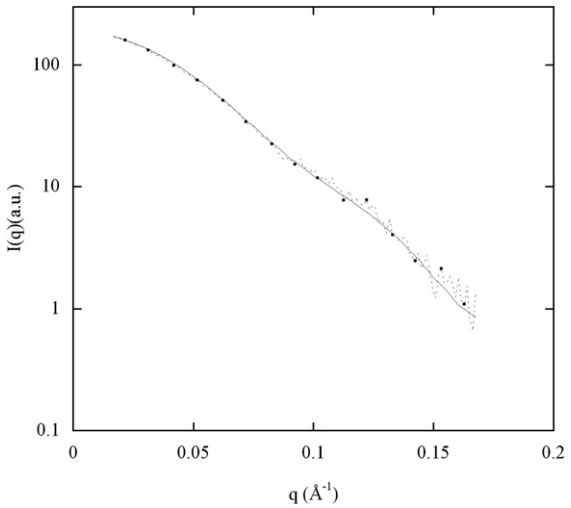

Figure 4. Comparison of the experimental scattering intensity of hLf (dotted line) with the scattering pattern calculated from the atomic coordinates of holo hLf (1B0L.pdb) using the program CRYSOL (continuous line).

complex, we recorded the SAXS pattern of the solution obtained using a 1:2 molar ratio without the purification step by HPLC. The resulting curve was almost identical to that of a 1:1 complex but exhibited a marked upward curvature at smaller angles (data not shown). This observation is an unambiguous indication of the presence of high molecular weight species that cannot be attributed to a complex with a higher stoichiometry but is most likely due to uncomplexed hLf aggregates.

We checked the stability of the 1:1 complex by eluting the protein mixture 6 h after preparation. The complex eluted at the same position and was characterized by the same SAXS pattern as the freshly prepared sample.

The scattering pattern of the hCp:hLf complex (Figure 2, continuous line) exhibits features quite different from those of purified hCp and hLf. The analysis of the Guinier region yields a radius of gyration of $R_g = 42.8(\pm 1)$ Å. From the $p(r)$ function (presented in Figure 3, continuous line), we calculated a value of the radius of gyration of 43.8(±0.3) Å, which is in good agreement with the value obtained from the Guinier approximation and a maximum dimension of the complex (D_{max}) of 150(±5) Å (see also Table 1). Finally, the $I(0)/c$ values (proportional to the molecular mass) of hCp, hLf and of the complex are in the expected ratios for a 1:1 complex (see Table 1).

Conformation in solution of the hCp:hLf complex

The *ab initio* DAM procedure (see Materials and Methods) used to determine the shape of the complex was run ten times yielding ten low-resolution models that are highly similar as shown by the low value of the mean normalized spatial discrepancy d of 0.58 ± 0.02. All models appear to be compatible with the 1:1 stoichiometry when superposing the high-resolution crystal structures of the isolated components over the low-resolution SAXS models of the complex. This is noteworthy in view of the absence of any assumption regarding the stoichiometry of the complex in the modeling procedure.

To obtain information on the mutual arrangement of the two proteins within the complex, we tried to fit the experimental scattering curve of the complex with the calculated one obtained after positional refinement of the crystal structures of pure hLf and pure hCp using the program SASREF.[48]

First we performed a complete six-dimensional search roto-translating the lactoferrin molecule without external constraints while keeping ceruloplasmin fixed in its original position. The resulting model (model A) determined by the rotation-translation matrix given in Table 2A, was characterized by a scattering pattern with a low χ-value against experimental data (1.51). In this model, the C-terminal region of hCp is in contact with the C-lobe of hLf (see Figure 5(a)).

Since previous studies[36,38] suggested that the basic N-terminal region of hLf is involved in the formation of the complex with hCp, we ran the program SASREF again while imposing an interaction of hCp with the hLf N-lobe (amino acid residues 2–31). The scattering curve of the resulting model (model B) is in equally good agreement with the experimental curve as that of model A ($\chi = 1.61$). The long axis of the hLf molecule is close to its position in model A, but its orientation is opposite, with the N-terminal region contacting hCp (see Figure 5(b) and Table 2B for the rotation-translation matrix). Therefore, SAXS alone cannot discriminate between these two models due to the very shape of hLf.

Finally, a validation of the methods came out from the superposition of the models independently obtained according to the two different procedures (namely, *ab initio* DAM procedure and fitting of the experimental curve of the complex with a position refinement of the crystal structures of isolated components with SASREF). The models superposed

Table 2. Transformation matrices obtained for the two models of the hLf:hCp complex starting from the atomic coordinates of the pdb files 1B0L.pdb (hLf) and 1KCW.pdb (hCp)

A. *Model A*[a]*: transformation matrix for 1B0L.pdb*			
−0.224611	−0.739598	−0.634464	135.307932
0.972692	−0.131098	−0.191528	−2.626136
0.058477	−0.660157	0.748848	32.144269
0.000000	0.000000	0.000000	1.000000
B. *Model B*[a]*: transformation matrix for 1B0L.pdb*			
−0.328213	−0.527389	0.783669	109.804464
−0.828879	0.558685	0.028832	−34.685209
−0.453030	−0.640103	−0.620509	40.766419
0.000000	0.000000	0.000000	1.000000

[a] For both models the transformation matrix of 1KCW.pdb, kept fixed, is the identity matrix.

Please cite this article as: Sabatucci, A. *et al.*, Structural Characterization of the Ceruloplasmin: Lactoferrin Complex in Solution, *J. Mol. Biol.* (2007), doi:10.1016/j.jmb.2007.05.089

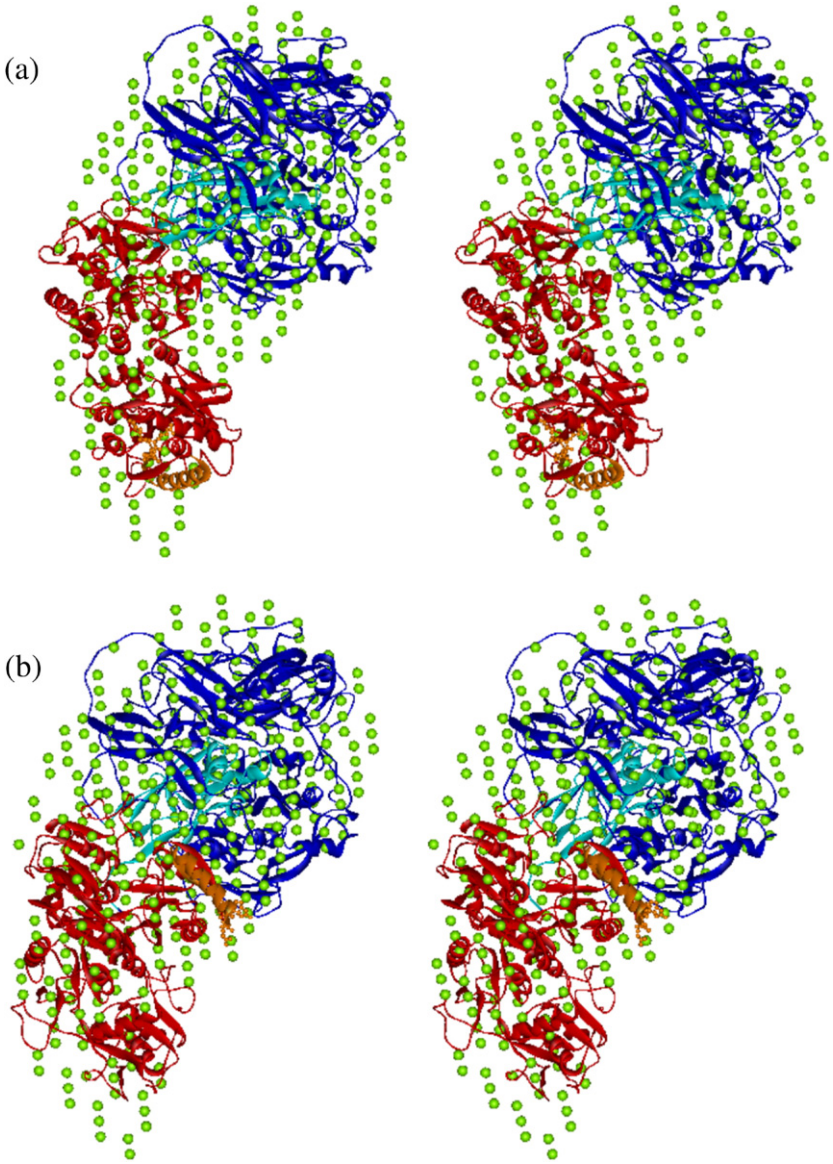

Figure 5. (a) Stereo view of the DAM structure of the hCp:hLf complex (green spheres) superposed to model A, obtained after positional refinement of the crystal structures of hCp and hLf using the program SASREF without any structural constraint. hCp is represented as a blue ribbon, the C-terminal domain 6 is cyan; hLf is represented as a red ribbon. The hLf N-terminal region (amino acid residues 1–31) is orange and the residues ^{2}R-R-R-R^{5} are drawn as ball and stick. (b) Stereo view of the DAM structure of the hCp:hLf complex superposed to the model B obtained from the crystal structures of hLf and hCp, imposing a close proximity of the hLf N-terminal region to the hCp surface. Notations as in (a).

with the program SUPCOMB overlap almost completely, as can be seen in Figure 5(a) and (b).

Discussion

Our results show that hCp and hLf are able to form a stable complex in solution with a 1:1 stoichiometry, which is in line with the data on the natural hCp:hLf complex isolated from breast milk.[36] Furthermore, our study indicates that the complex is sensitive to buffer composition. Indeed, phosphate buffer induces the formation of high molecular weight aggregates with a scattering pattern characterized by a marked upward curvature close to the origin. Tris-HCl buffer favors the formation of a stable monodisperse complex with a well-defined 1:1 stoichiometry whatever the hCp:hLf molar ratio used. These data are supported by basic physico-chemical studies showing that phosphate buffer has a kosmotropic effect,[49] while the organic buffer Tris has a chaotropic effect in solution.[50]

All *ab initio* models derived from the SAXS pattern of the hCp:hLf complex using DAMMIN are very similar as shown by the low NSD values, indicating the near unicity of this low resolution shape. These models provide a nice envelope to models obtained using rigid-body refinement of the relative position of both proteins, thereby confirming the robustness of the *ab initio* solution. Furthermore, the scattering patterns of the rigid-body models yield excellent fits to the experimental data. This suggests that the global conformations of the two partners do not undergo any major changes upon complex formation. These results complement a previously published CD analysis in which the experimental spectrum of the hCp:hLf complex in the near-UV region appeared to be well approximated by the arithmetic sum of hCp and hLf spectra.[35]

Rigid-body modeling of the complex using the two crystal structures of the partners allows us to determine the mutual arrangement of the proteins within the hCp:hLf complex.

Please cite this article as: Sabatucci, A. *et al.*, Structural Characterization of the Ceruloplasmin: Lactoferrin Complex in Solution, *J. Mol. Biol.* (2007), doi:10.1016/j.jmb.2007.05.089

Firstly, our results strongly suggest that the C-terminal region of hCp is involved in the interaction with hLf, since hCp shows the same orientation with respect to hLf in both models A and B. This result agrees with previous studies indicating that the C-terminal region (domain 6) of hCp is involved in the interaction with protamine, the amino acid sequence of which has homology with the N terminus of Lf.[39] It is also in line with the data on direct involvement of the C-terminal part of hCp in contact with protein C[51] and ferritin,[52] though the latter proteins are bound to the ^{1028}HAGMETTYTV^{1037} stretch in hCP that is most likely different from the Lf binding site.[36]

Regarding the orientation of hLf with respect to hCp, the symmetry of the protein did not allow us, through an analysis of the SAXS data, to discriminate between the involvement of the C-terminal or the N-terminal lobe. However, heparin, which essentially interacts with the N-terminal arginine stretch ^{2}R-R-R-R^{5} of hLf,[28] has been shown to cause the dissociation of the complex *in vitro*[38] pointing to the electrostatic character of the interaction between the two proteins. This notion got further support from the biochemical data collected on the interaction of the cationic N-terminal region of hLf with the negatively charged C-terminal domain of hCp.[37] A recent study of the likely sites in hLf for interaction with hCp also indicated that the N-terminal ^{2}R-R-R-R^{5} stretch is the most probable candidate.[36] These results favor the involvement of the N-lobe in the interaction and therefore model B as being more plausible.

Finally, we would like to point out that using the most recent versions of several protein–protein docking programs to simulate the 1:1 hCp:hLf interaction (data not shown), the best-ranking models obtained had volumes much smaller than the one calculated from the SAXS data, and quite different shapes. They often involve both the C-lobe and N-lobe of hLf in the interaction forming, as a result, a much tighter complex with a more extensive interface. Such models are clearly incompatible with our experimental data. These discrepancies underline *a contrario*, the advantage to be expected from the use of SAXS in the framework of data-driven docking analysis.[45] Taken together, our results confirm the validity of the chosen SAXS approach that, applied in a synergistic way with other biochemical and biophysical techniques, allows us not only to establish the stoichiometry of the hCp:hLf complex in solution but also to propose a model for the mutual arrangement of the two proteins.

Materials and Methods

Protein purification

All reagents were of analytical grade. HLf from skimmed breast milk was purified and then saturated with iron as described.[35]

Iron saturation of the hLf samples was checked spectrophotometrically by measuring the absorbance ratio A_{450}/A_{280}. A ratio >0.037 was obtained for iron-saturated samples. A saturation of about 90% was measured for all samples used thereafter.

Stable hCp was purified as described.[39]

Protein concentrations were assessed both spectrophotometrically determining the absorbance at 280 nm and using the Bradford method.[53] The extinction coefficients adopted are $\varepsilon^{0.1\%}_{280}=1.46$ mg^{-1} cm^2 for hLf[54] and $\varepsilon^{0.1\%}_{280}=1.61$ mg^{-1} cm^2 for hCp.[55] Where needed, for the complex, an extinction coefficient of $\varepsilon^{0.1\%}_{280}=1.5$ mg^{-1} cm^2 was calculated, as an average of the extinction coefficients of hLf and hCp. The assumption was made that the extinction coefficients were not affected by complex formation.

SE-HPLC measurements

SE-HPLC measurements were performed on a PE Series 200 System (Perkin Elmer Life and Analytical Sciences, Boston, MA) using a Shodex-Protein SB-804 column (Showa Denko K.K., Kawasaki, Japan), which allows a separation range from 10 to about 800 kDa. Purified hLf was exhaustively dialyzed against the chosen buffer before SE-HPLC analysis. To find the best conditions ensuring the monodispersity of the sample we varied the buffer used (50 mM sodium phosphate and 50 mM Tris-HCl), pH (7.0, 7.2 and 7.5) and salt content (none or 100 mM NaCl). All parameter combinations were investigated. The hCp:hLf complex was obtained by directly mixing hCp and hLf solutions using a hCp:hLf molar ratio of either 1:2 or 1:1. Both proteins were extensively dialyzed against the same buffer before mixing.

The SE-HPLC column was calibrated using the following molecular mass standards (Pharmacia, Uppsala, Sweden): bovine serum albumin (67 kDa), aldolase (158 kDa), catalase (232 kDa), ferritin (440 kDa) (data not shown).

SAXS measurements and data processing

SAXS measurements were performed using the D24 beam-line at the LURE synchrotron radiation facility (Orsay, France) with a monochromatic X-ray beam adjusted to a wavelength of 1.488 Å (absorption K-edge of Nickel). The measuring cell under vacuum[56] was kept at constant temperature (6 °C) during measurements.

Eight frames of 100 s each were recorded and averaged after visual inspection for radiation damage (none was found). The scattering intensities were measured over the q-range $q_{min}=0.01$ Å^{-1} $q_{max}=0.20$ Å^{-1} for holo hLf and $q_{min}=0.01$ Å^{-1} $q_{max}=0.25$ Å^{-1} for the complex ($q=(4\pi/\lambda)\sin\theta$, 2θ being the scattering angle).

The beam intensity was calibrated using reference protein samples with known molecular mass: native hemocyanin (Hc) from *Panulirus interruptus* (450 kDa) and native Hc from *Carcinus aestuarii* (900 kDa) at a concentration of 5 mg/ml in 50 mM Tris-HCl buffer (pH 7.0) containing 20 mM $CaCl_2$. Each sample was collected from SE-HPLC and immediately analyzed by SAXS. Purified hLf was measured at a concentration of 2.7 mg/ml. No measurement at higher concentrations was possible due to the formation of high molecular mass aggregates. The hCp:hLf complex was measured at a complex concentration of 1.6 and 23.3 mg/ml. The measurement conditions for holo hCp have already been described.[16]

The radius of gyration (R_g) and the molecular mass of the proteins were calculated applying the Guinier

Please cite this article as: Sabatucci, A. *et al.*, Structural Characterization of the Ceruloplasmin: Lactoferrin Complex in Solution, *J. Mol. Biol.* (2007), doi:10.1016/j.jmb.2007.05.089

approximation[57] to the low-q region of the scattering pattern ($R_g x q<1.3$):

$$\ln\frac{I(q)}{c} = \ln\frac{I(0)}{c} - \left(\frac{R_g^2}{3}\right)q^2 \quad (1)$$

where $I(0)/c$,the zero-angle intensity, is directly proportional to the molecular mass of the protein, after proper calibration (see above).

The distance distribution function $p(r)$, which gives the distribution of distances between any two volume elements within one particle, was determined using the indirect Fourier transform method as implemented in the program package GNOM.[58]

This function provides, beyond the maximum diameter D_{max} of the particle, an alternative estimate of the radius of gyration, derived through the relationship:

$$Rg^2 = \frac{\int r^2 p(r)dr}{2\int p(r)dr} \quad (2)$$

Scattering patterns from the crystal structure of both hLf and hCp were calculated and fitted against experimental data using CRYSOL.[59] For hLf we used the atomic coordinates of recombinant human holo diferric lactoferrin at 2.2 Å resolution (1B0L.pdb).[47] In the case of holo hCp, we used the PDB file 1kcw,[10] taking into account the contribution of the carbohydrate chains to scattering as described by Vachette *et al*.[16]

The *ab initio* model of the complex was obtained using the dummy atom model method (DAM) as implemented in the program DAMMIN.[60] The procedure yields an approximation of the shape scattering curve (i.e. the scattering due to the excluded volume of the particle filled by constant density) and thus a low-resolution model of the particles. Ten independent calculations have been performed. Their consistency was checked out with the program SUPCOMB[61] that, starting from an inertia-axes alignment, minimizes the normalized spatial discrepancy (NSD) d between two three-dimensional objects. The final value of d provides a quantitative estimate of similarity between the two objects: in general, when $d<1$, two objects can be considered similar. The model with the lowest discrepancy against the experimental data has been chosen as representative of the low-resolution structure of the complex in solution. This modeling approach is free from any prior assumption regarding the stoichiometry of the complex.

The mutual arrangement of hLF and hCp within the 1:1 complex was determined using the program SASREF.[48] One protein is moved as a rigid body with respect to the other one following a simulated annealing protocol so as to minimize the discrepancy between the experimental scattering data and the calculated curve of the complex.

No structural constraint was used for the calculation of model A, while, for model B, a maximal distance of 7 Å between the C^{α} atoms of specific residues of hCp and hLf was imposed.

Acknowledgements

This work was supported by the 5th Framework Program of the European Commission "Access to Research Infrastructures", project no. BD 005-00 carried out at LURE. Financial support by the Ministero Politiche Agricole e Forestali ("FORMINNOVA" 2001 to E.D.), by Ministero dell'Università e della Ricerca (PRIN 2005 to E.D.), by RFBR grants No. 06-04-48602 and No. 05-04-48765, and by the University of Padova (Progetto di Ateneo CPDA051777 to M.B.) are also gratefully acknowledged.

References

1. Osaki, S., Johnson, D. A. & Frieden, E. (1966). The possible significance of the ferrous oxidase activity of ceruloplasmin in normal human serum. *J. Biol. Chem.* **241**, 2746–2751.
2. Osaki, S., Johnson, D. A. & Frieden, E. (1971). The mobilization of iron from the perfused mammalian liver by a serum copper enzyme, ferroxidase I. *J. Biol. Chem.* **246**, 3018–3023.
3. Frieden, E. & Hsieh, H. S. (1976). The biological role of ceruloplasmin and its oxidase activity. *Advan. Exp. Med. Biol.* **74**, 505–529.
4. Hellman, N. E. & Gitlin, J. D. (2002). Ceruloplasmin metabolism and function. *Annu. Rev. Nutr.* **22**, 439–458.
5. Vassiliev, V., Harris, Z. L. & Zatta, P. (2005). Ceruloplasmin in neurodegenerative diseases. *Brain Res. Brain Res. Rev.* **49**, 633–640.
6. Kosman, D. J. (2002). FET3P, ceruloplasmin, and the role of copper in iron metabolism. *Advan. Protein Chem.* **60**, 221–269.
7. Taylor, A. B., Stoj, C. S., Ziegler, L., Kosman, D. J. & Hart, P. J. (2005). The copper-iron connection in biology: structure of the metallo-oxidase Fet3p. *Proc. Natl Acad. Sci. USA*, **102**, 15459–15464.
8. Takahashi, N., Bauman, R. A., Ortel, T. L., Dwulet, F. E., Wang, C. C. & Putnam, F. W. (1983). Internal triplication in the structure of human ceruloplasmin. *Proc. Natl Acad. Sci. USA*, **80**, 115–119.
9. Ortel, T. L., Takahashi, N. & Putnam, F. W. (1984). Structural model of human ceruloplasmin based on internal triplication, hydrophilic/hydrophobic character, and secondary structure of domains. *Proc. Natl Acad. Sci. USA*, **81**, 4761–4765.
10. Zaitseva, I., Zaitsev, V., Card, G., Moshkov, K., Bax, B., Ralph, A. & Lindley, P. (1996). The X-ray structure of human serum ceruloplasmin at 3.1 Å: nature of the copper centres. *J. Biol. Inorg. Chem.* **1**, 15–23.
11. Ryden, L. (1984). Ceruloplasmin. In *Copper Proteins and Copper Enzymes* (Lontie, R., ed), pp. 37–100, CRC Press, Boca Raton, Florida, USA.
12. Messerschmidt, A., Ladenstein, R., Huber, R., Bolognesi, M., Avigliano, L., Petruzzelli, R. *et al.* (1992). Refined crystal structure of ascorbate oxidase at 1.9 Å resolution. *J. Mol. Biol.* **224**, 179–205.
13. Messerschmidt, A. & Huber, R. (1990). The blue oxidases, ascorbate oxidase, laccase and ceruloplasmin. Modelling and structural relationships. *Eur. J. Biochem.* **187**, 341–352.
14. Messerschmidt, A. (1997). Spatial structures of ascorbate oxidase, laccase and related proteins: implications for the catalytic mechanism. In *Multi-opper Oxidases* (Messerschmidt, A., ed), pp. 23–79, World Scientific, Singapore.
15. Ducros, V., Brzozowski, A. M., Wilson, K. S., Ostergaard, P., Schneider, P., Svendson, A. & Davies,

G. J. (2001). Structure of the laccase from Coprinus cinereus at 1.68 Å resolution: evidence for different 'type 2 Cu-depleted' isoforms. *Acta Crystallog. sect. D*, **57**, 333–336.
16. Vachette, P., Dainese, E., Vasyliev, V. B., Di Muro, P., Beltramini, M., Svergun, D. I. *et al.* (2002). A key structural role for active site type 3 copper ions in human ceruloplasmin. *J. Biol. Chem.* **277**, 40823–40831.
17. Anderson, B. F., Baker, H. M., Dodson, E. J., Norris, G. E., Rumball, S. V., Waters, J. M. & Baker, E. N. (1987). Structure of human lactoferrin at 3.2-Å resolution. *Proc. Natl Acad. Sci. USA*, **84**, 1769–1773.
18. Haridas, M., Anderson, B. F., Baker, H. M., Norris, G. E. & Baker, E. N. (1994). X-ray structural analysis of bovine lactoferrin at 2.5 A resolution. *Advan. Exp. Med. Biol.* **357**, 235–238.
19. Baker, H. M. & Baker, E. N. (2004). Lactoferrin and iron: structural and dynamic aspects of binding and release. *Biometals*, **17**, 209–216.
20. Naot, D., Grey, A., Reid, I. R. & Cornish, J. (2005). Lactoferrin–a novel bone growth factor. *Clin. Med. Res.* **3**, 93–101.
21. Schryvers, A. B., Bonnah, R., Yu, R. H., Wong, H. & Retzer, M. (1998). Bacterial lactoferrin receptors. *Advan. Exp. Med. Biol.* **443**, 123–133.
22. Siebert, P. D. & Huang, B. C. (1997). Identification of an alternative form of human lactoferrin mRNA that is expressed differentially in normal tissues and tumor-derived cell lines. *Proc. Natl Acad. Sci. USA*, **94**, 2198–2203.
23. Sakamoto, K., Ito, Y., Mori, T. & Sugimura, K. (2006). Interaction of human lactoferrin with cell adhesion molecules through RGD motif elucidated by lactoferrin-binding epitopes. *J. Biol. Chem.* **281**, 24472–24478.
24. de Lillo, A., Tejerina, J. M. & Fierro, J. F. (1992). Interaction of calmodulin with lactoferrin. *FEBS Letters*, **298**, 195–198.
25. Lampreave, F., Pineiro, A., Brock, J. H., Castillo, H., Sanchez, L. & Calvo, M. (1990). Interaction of bovine lactoferrin with other proteins of milk whey. *Int. J. Biol. Macromol.* **12**, 2–5.
26. Watanabe, T., Nagura, H., Watanabe, K. & Brown, W. R. (1984). The binding of human milk lactoferrin to immunoglobulin A. *FEBS Letters*, **168**, 203–207.
27. Wong, H. & Schryvers, A. B. (2003). Bacterial lactoferrin-binding protein A binds to both domains of the human lactoferrin C-lobe. *Microbiology*, **149**, 1729–1737.
28. van Berkel, P. H., Geerts, M. E., van Veen, H. A., Mericskay, M., de Boer, H. A. & Nuijens, J. H. (1997). N-terminal stretch Arg2, Arg3, Arg4 and Arg5 of human lactoferrin is essential for binding to heparin, bacterial lipopolysaccharide, human lysozyme and DNA. *Biochem. J.* **328**, 145–151.
29. Mann, D. M., Romm, E. & Migliorini, M. (1994). Delineation of the glycosaminoglycan-binding site in the human inflammatory response protein lactoferrin. *J. Biol. Chem.* **269**, 23661–23667.
30. Wu, H. F., Monroe, D. M. & Church, F. C. (1995). Characterization of the glycosaminoglycan-binding region of lactoferrin. *Arch. Biochem. Biophys.* **317**, 85–92.
31. van Veen, H. A., Geerts, M. E., van Berkel, P. H. & Nuijens, J. H. (2002). Analytical cation-exchange chromatography to assess the identity, purity, and N-terminal integrity of human lactoferrin. *Anal. Biochem.* **309**, 60–66.
32. Legrand, D., van Berkel, P. H., Salmon, V., van Veen, H. A., Slomianny, M. C., Nuijens, J. H. & Spik, G. (1998). Role of the first N-terminal basic cluster of human lactoferrin (R2R3R4R5) in the interactions with the Jurkat human lymphoblastic T-cells. *Advan. Exp. Med. Biol.* **443**, 49–55.
33. Ziere, G. J., Bijsterbosch, M. K. & van Berkel, T. J. (1993). Removal of 14 N-terminal amino acids of lactoferrin enhances its affinity for parenchymal liver cells and potentiates the inhibition of beta- very low density lipoprotein binding. *J. Biol. Chem.* **268**, 27069–27075.
34. Yazidi-Belkoura, I., Legrand, D., Nuijens, J., Slomianny, M. C., van Berkel, P. & Spik, G. (2001). The binding of lactoferrin to glycosaminoglycans on enterocyte-like HT29-18-C1 cells is mediated through basic residues located in the N-terminus. *Biochim. Biophys. Acta*, **1568**, 197–204.
35. Zakharova, E. T., Shavlovski, M. M., Bass, M. G., Gridasova, A. A., Pulina, M. O., De, F., V. *et al.* (2000). Interaction of lactoferrin with ceruloplasmin. *Arch. Biochem. Biophys.* **374**, 222–228.
36. Sokolov, A. V., Pulina, M. O., Zakharova, E. T., Susorova, A. S., Runova, O. L., Kolodkin, N. I. & Vasilyev, V. B. (2006). Identification and isolation from breast milk of ceruloplasmin-lactoferrin complex. *Biochemistry (Mosc.)*, **71**, 160–166.
37. Sokolov, A. V., Pulina, M. O., Zakharova, E. T., Shavlovski, M. M. & Vasilyev, V. B. (2005). Effect of lactoferrin on the ferroxidase activity of ceruloplasmin. *Biochemistry (Mosc.)*, **70**, 1015–1019.
38. Pulina, M. O., Zakharova, E. T., Sokolov, A. V., Shavlovski, M. M., Bass, M. G., Solovyov, K. V., Kokryakov, V. N. & Vasilyev, V. B. (2002). Studies of the ceruloplasmin-lactoferrin complex. *Biochem. Cell Biol.* **80**, 35–39.
39. Sokolov, A. V., Zakharova, E. T., Shavlovskii, M. M. & Vasil'ev, V. B. (2005). Isolation of stable human ceruloplasmin and its interaction with salmon protamine. *Bioorg. Khim.* **31**, 269–279.
40. Vachette, P., Koch, M. H. & Svergun, D. I. (2003). Looking behind the beamstop: X-ray solution scattering studies of structure and conformational changes of biological macromolecules. *Methods Enzymol.* **374**, 584–615.
41. Dainese, E., Sabatucci, A. & Cozzani, I. (2003). Small angle X-ray scattering: A powerful tool to analyze protein conformation in solution. *Curr. Org. Chem.* **9**, 1781–1800.
42. Higurashi, T., Hiragi, Y., Ichimura, K., Seki, Y., Soda, K., Mizobata, T. & Kawata, Y. (2003). Structural stability and solution structure of chaperonin GroES heptamer studied by synchrotron small-angle X-ray scattering. *J. Mol. Biol.* **333**, 605–620.
43. Zhang, W., Hirshberg, M., McLaughlin, S. H., Lazar, G. A., Grossmann, J. G., Nielsen, P. R. *et al.* (2004). Biochemical and structural studies of the interaction of Cdc37 with Hsp90. *J. Mol. Biol.* **340**, 891–907.
44. Gralle, M., Oliveira, C. L., Guerreiro, L. H., McKinstry, W. J., Galatis, D., Masters, C. L. *et al.* (2006). Solution conformation and heparin-induced dimerization of the full-length extracellular domain of the human amyloid precursor protein. *J. Mol. Biol.* **357**, 493–508.
45. van Dijk, A. D., Boelens, R. & Bonvin, A. M. (2005). Data-driven docking for the study of biomolecular complexes. *FEBS J.* **272**, 293–312.
46. Mantel, C., Miyazawa, K. & Broxmeyer, H. E. (1994). Physical characteristics and polymerization during iron saturation of lactoferrin, a myelopoietic regulatory molecule with suppressor activity. *Advan. Exp. Med. Biol.* **357**, 121–132.
47. Sun, X. L., Baker, H. M., Shewry, S. C., Jameson, G. B. & Baker, E. N. (1999). Structure of recombinant

Please cite this article as: Sabatucci, A. *et al.*, Structural Characterization of the Ceruloplasmin: Lactoferrin Complex in Solution, *J. Mol. Biol.* (2007), doi:10.1016/j.jmb.2007.05.089

human lactoferrin expressed in *Aspergillus awamori*. *Acta Crystallog. sect. D*, **55**, 403–407.
48. Petoukhov, M. V. & Svergun, D. I. (2005). Global rigid body modeling of macromolecular complexes against small-angle scattering data. *Biophys. J.* **89**, 1237–1250.
49. Cacace, M. G., Landau, E. M. & Ramsden, J. J. (1997). The Hofmeister series: salt and solvent effects on interfacial phenomena. *Quart. Rev. Biophys.* **30**, 241–277.
50. Washabaugh, M. W. & Collins, K. D. (1986). The systematic characterization by aqueous column chromatography of solutes which affect protein stability. *J. Biol. Chem.* **261**, 12477–12485.
51. Walker, F. J. & Fay, P. J. (1990). Characterization of an interaction between protein C and ceruloplasmin. *J. Biol. Chem.* **265**, 1834–1836.
52. Juan, S. H. & Aust, S. D. (1998). Studies on the interaction between ferritin and ceruloplasmin. *Arch. Biochem. Biophys.* **355**, 56–62.
53. Bradford, M. M. (1976). A rapid and sensitive method for the quantitation of microgram quantities of protein utilizing the principle of protein-dye binding. *Anal. Biochem.* **72**, 248–254.
54. Masson, P. L. (1970). In *La Lactoferrine. Proteine des Secretions Externes et des Leucocytes Neutrophiles*. Editions Arscia S.A, Brussels.
55. De Filippis, V., Vassiliev, V. B., Beltramini, M., Fontana, A., Salvato, B. & Gaitskhoki, V. S. (1996). Evidence for the molten globule state of human apoceruloplasmin. *Biochim. Biophys. Acta*, **1297**, 119–123.
56. Dubuisson, J. M., Decamps, T. & Vachette, P. (1997). Improved signal-to-background ratio in small-angle X-ray scattering experiments with synchrotron radiation using an evacuated cell for solutions. *J. Appl. Crystallog.* **30**, 49–54.
57. Guinier, A. & Fournet, G. (1955). *Small Angle Scattering of X-rays.* Wiley, New York.
58. Svergun, D. I. (1992). Determination of the regularization parameter in indirect-transform methods using perceptual criteria. *J. Appl. Crystallog.* **25**, 495–503.
59. Svergun, D. I., Barberato, C. & Koch, M. H. (1995). Crysol-a program to evaluate X-ray solution scattering of biological macromolecules from atomic coordinates. *J. Appl. Crystallog.* **28**, 768–773.
60. Svergun, D. I. (1999). Restoring low resolution structure of biological macromolecules from solution scattering using simulated annealing. *Biophys. J.* **76**, 2879–2886.
61. Kozin, M. B. & Svergun, D. I. (2001). Automated matching of high- and low-resolution structural models. *J. Appl. Crystallog.* **34**, 33–41.

Edited by R. Huber

(Received 9 February 2007; received in revised form 24 May 2007; accepted 29 May 2007)